UNIVERSITY *of York*

This is a repository copy of *An emergent functional parcellation of the temporal cortex*.

Article:

White Rose
university consortium
Universities of Leeds, Sheffield & York

eprints@whiterose.ac.uk
https://eprints.whiterose.ac.uk/

An emergent functional parcellation of the temporal cortex

CrossMark

Rebecca L. Jackson[1], Claude J. Bajada[1], Grace E. Rice, Lauren L. Cloutman, Matthew A. Lambon Ralph[*]

Neuroscience and Aphasia Research Unit (NARU), Division of Neuroscience & Experimental Psychology, School of Biological Sciences (Zochonis Building), University of Manchester, M13 9PL, UK

ARTICLE INFO

ABSTRACT

The temporal lobe has been associated with various cognitive functions which include memory, auditory cognition and semantics. However, at a higher level of conceptualisation, all of the functions associated with the temporal lobe can be considered as lying along one major axis; from modality-specific to modality-general processing. This paper used a spectral reordering technique on resting-state and task-based functional data to extract the major organisational axis of the temporal lobe in a bottom-up, data-driven fashion. Independent parcellations were performed on resting-state scans from 71 participants and active semantic task scans from 23 participants acquired using dual echo gradient echo planar imaging in order to preserve signal in inferior temporal cortex. The resulting organisational axis was consistent (over dataset and hemisphere) and progressed from superior temporal gyrus and posterior inferior temporal cortex to ventrolateral anterior temporal cortex. A hard parcellation separated a posterior (superior temporal and posterior fusiform and inferior temporal gyri) and an anterior cluster (ventrolateral anterior temporal lobe). The functional connectivity of the hard clusters supported the hypothesis that the connectivity gradient separated modality-specific and modality-general regions. This hypothesis was then directly tested by performing a VOI analysis upon an independent semantic task-based data set including auditory and visually presented stimuli. This confirmed that the ventrolateral anterior aspects of the temporal lobe are associated with modality-general processes whilst posterior and superior aspects are specific to certain modalities, with the posterior inferior subregions involved in visual processes and superior regions involved in audition.

Introduction

Sensory information is first processed in modality-specific sensory and association cortices before converging in multimodal association areas (Mesulam, 1998; Plaut, 2002; Braga et al., 2017). This process is critical for semantic cognition and may underlie a multitude of cognitive processes (Mesulam, 1998; Patterson et al., 2007; Lambon Ralph, 2014; Lambon Ralph et al., 2017). The temporal lobe is an important site for this convergence, as it includes primary auditory cortex as well as auditory and visual association areas. Tracer studies and intra-cortical electrode recordings in non-human primates have shown a hierarchy of visual processing extending anteriorly from occipital cortex along temporal cortex (Felleman and Van Essen, 1991). The posterolateral inferotemporal area in the macaque and the posterior fusiform gyrus (FG) in humans receive visual input from the occipital lobe and are thought to be responsible for combining

visual features to form representations of complex shapes (Halgren et al., 1997; Kanwisher et al., 1997b; Mesulam, 1998; Felleman and Van Essen, 1991). However, these shapes are divorced from meaning until anterior inferior temporal regions (Gross et al., 1972; Bell et al., 2009; Desimone, 1991; Kriegeskorte et al., 2008; Kanwisher et al., 1997a). A distinct auditory stream progresses anteriorly along the superior temporal gyrus (STG) showing a similar gradient of complexity (Rauschecker and Scott, 2009). Anterior STG regions encode complex auditory sequences in various non-human primates and increasingly reflect higher-order properties of language in humans (Rauschecker and Scott, 2009; Scott et al., 2000; Tian et al., 2001; Colombo et al., 1996).

The primate literature suggests multimodal association areas exist in lateral temporal cortex and portions of the parahippocampal gyrus (Mesulam, 1998). The existence of a multimodal 'hub' for semantic cognition has been demonstrated in humans. Semantic dementia

patients experience a selective and progressive deterioration of multi-modal semantic representations associated with atrophy and hypome-tabolism of the ventrolateral anterior temporal lobe (ATL; Patterson et al., 2007; Mion et al., 2010; Acosta-Cabronero et al., 2011; Lambon Ralph, 2014). The importance of the ventrolateral ATL in multimodal semantic cognition has been confirmed with PET, MEG and cortical grid electrodes as well as fMRI studies designed to reduce artefact-related signal loss within inferior temporal regions (Binney et al., 2010; Visser et al., 2012; Visser and Lambon Ralph, 2011; Jackson et al., 2015; Halai et al., 2014; Marinkovic et al., 2003; Devlin et al., 2000; Shimotake et al., 2014; Chen et al., 2016; Abel et al., 2015). Tractography analysis of the human temporal lobe (Binney et al., 2012) confirms the appropriate structure for a graded convergence of auditory and visual information in the ATL (Plaut, 2002). This convergence occurs laterally and rostrally along the temporal lobe (Binney et al., 2012; Binder et al., 2009). Indeed, the ventrolateral ATL regions may be strategically remote from all input sources, allowing extraction of high-order multimodal statistical structures without bias towards a specific modality (Binney et al., 2012; Lambon Ralph, 2014; Rice et al., 2015b, 2015a; Lambon Ralph et al., 2017).

The distinction between modality-specific and modality-general regions appears to be critical in the functional organisation of the temporal lobe. Therefore, it should be possible for this distinction to emerge from the data in a bottom up fashion. Previous studies have sought to parcellate the whole brain using resting-state data (e.g. Wig et al., 2014). However, these results are susceptible to the signal loss and distortion in inferior temporal cortex, an issue highlighted in previous seed-based and whole-brain connectivity studies (Wig et al., 2014; Zuo et al., 2012; Ding et al., 2009; Yeo et al., 2011). Here we performed a parcellation of the temporal lobe based on both resting-state and active-task fMRI data acquired using a dual echo technique designed to reduce signal loss and distortion in the ATL (Halai et al., 2014). A prominent distinction between modality-specific and mod-ality-general regions was predicted and the interpretation of the resulting regions was directly tested using independent task data employing a manipulation of visual and auditory presentation.

Materials and methods

Participants

Two sets of data were used for the functional parcellation: a set of resting-state data and data from an explicit semantic decision task. We tested the functional nature of the clusters identified in the data-driven parcellations using a third, independent fMRI dataset. This employed a semantic task engaging multiple modalities, thus allowing us to test the prediction that the clusters are differentiated on the basis of modality-specific and modality-general processing. Specifically, the resting-state data was collected from 78 participants (57 female, age range 18–42, average age 24.71 years, standard deviation 5.49 years). Seed-based functional connectivity analysis within this set of dual-echo EPI resting-state data have been reported previously (Jackson et al., 2016) as well as a graph theoretical analysis of the functional connectivity between temporal, parietal and frontal regions (Jung et al., 2016). Of these 78 participants, 24 also completed an active semantic task employing dual gradient echo fMRI, also reported previously (15 female, age range 20–42, average age 25.63 years; Jackson et al., 2015). These datasets were used to create two independent functional parcellations. A further 20 participants completed an independent dual gradient echo fMRI study of auditory and visual semantic decisions also reported previously (16 female; age range=20–42, average age=26.6 years; Rice et al., in preparation for publication). This dataset was used in the VOI analysis only. Participants were strongly right handed (minimum laterality quotient 50, average 85.85, standard deviation 14.91 on the Edinburgh Handedness Inventory; Oldfield, 1971). Participant's vision was nor-

mal or corrected-to-normal. All participants gave informed consent and the study was approved by the local ethics board.

Procedure

Scanning was conducted using a Phillips Achieve 3.0T system with 32 channel SENSE coil with a sense factor of 2.5. Noise cancelling Mk II+ headphones were worn inside the scanner (MR Confon, Magdeburg, Germany). A structural reference was obtained with an in-plane resolution of .938 and slice thickness of 1.173. Whole brain coverage was obtained with a field of view of 240×240 mm, which was tilted up to 45° off the AC-PC line to reduce the effect of ghosting on the temporal pole. The TR was 2.8 with a flip angle of 85°, resolution matrix of 80×80, reconstructed voxel size of 3 mm and slice thickness of 4 mm. 130 volumes were collected over 6.25 min for the resting-state scan. The active task data consisted of three runs each lasting 10 min and including 211 volumes. The imaging parameters were identical for the resting-state and active task scans used in the functional parcellation, as well as for the independent multimodal semantic task data used for the VOI analysis.

A dual gradient echo EPI technique was employed. This involves parallel acquisition at a short echo (12 ms) leading to a reduction in signal loss in areas of high magnetic susceptibility and a standard long echo (35 ms) to maintain high contrast sensitivity throughout the brain. The results from the two echoes were combined using linear summation, previously shown to be optimal (Poser et al., 2006; Halai et al., 2014). The resultant reduction in signal dropout is greatest within inferior temporal and orbitofrontal regions, reducing the impact of signal loss within the temporal lobe on the parcellation results (Poser and Norris, 2007, 2009; Halai et al., 2014). The preservation of good TSNR values in the inferior temporal regions in the resting-state and task data used here has been reported previously (Jackson et al., 2015, 2016). Although the signal is high there will always be variation in signal especially around problematic regions. To show that these variations are not causing the parcellation results, the gradient of change in the signal has been included in Supplementary Fig. 1. The signal changes principally in an inferior to superior axis that does not match the gradient of connectivity change.

During the resting-state scans participants were asked to fixate on a cross and lie still (Van Dijk et al., 2012). The active task data included a semantic task, a baseline task and rest periods. Stimuli were presented in mini-blocks of 15 s each containing 3 trials. The semantic task involved a triad judgement in which participants were asked to match a probe word (e.g., HEN) to the more semantically-related of two choice words (e.g. CAGE is more related than ROBE). In the baseline task, participants were asked to decide which of two letter strings (contain-ing Greek and Roman letters) overlapped the most with the probe string. For example, 'bqwcHΨz' is a better match to '##HΨz##' than 'cHΨdLXQ' is. Both tasks started with a central fixation cross presented for 1000ms followed by presentation of the stimuli for 4000 ms. During this time participants responded by pressing one of two buttons. The independent task data employed for the VOI analysis only, included people, landmarks and animals presented auditorily (spoken names) or visually (pictures). For both participants made a semantic decision ('Is the stimuli European or not?') and responded by button press.

Data analysis

Preprocessing

The effects of motion can greatly impact functional connectivity results, principally by causing distance-dependent increases in con-nectivity (Power et al., 2014; Van Dijk et al., 2012; Yan et al., 2013; Friston et al., 1996). For this reason great care was taken to account for motion when preprocessing both the resting-state and task data prior to the functional parcellation. The resting-state data was pre-processed
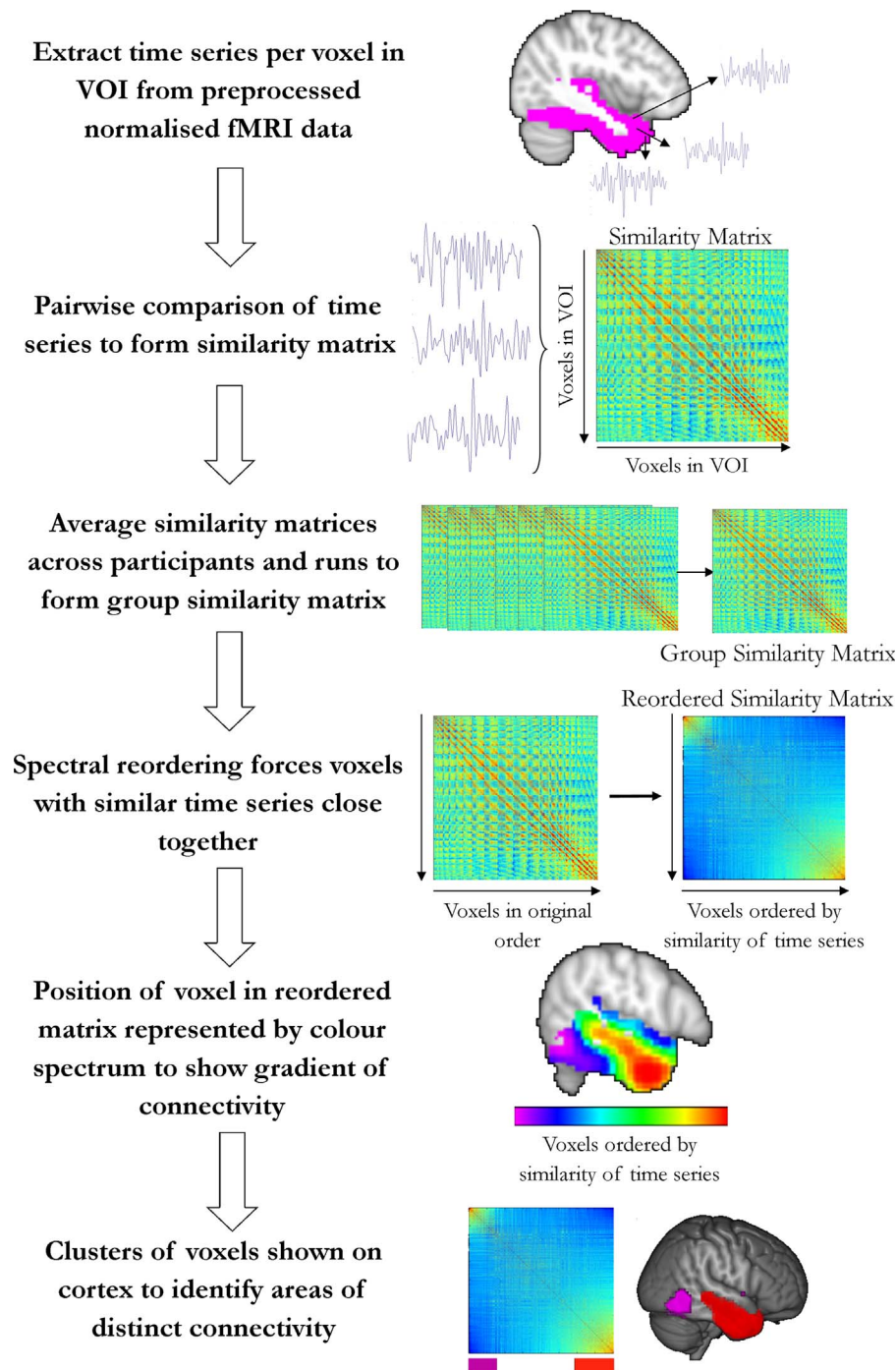
Extract time series per voxel in VOI from preprocessed normalised fMRI data

Pairwise comparison of time series to form similarity matrix

Similarity Matrix

Voxels in VOI

Voxels in VOI

Average similarity matrices across participants and runs to form group similarity matrix

Group Similarity Matrix

Reordered Similarity Matrix

Spectral reordering forces voxels with similar time series close together

Voxels in original order

Voxels ordered by similarity of time series

Position of voxel in reordered matrix represented by colour spectrum to show gradient of connectivity

Voxels ordered by similarity of time series

Clusters of voxels shown on cortex to identify areas of distinct connectivity

Fig. 1. The parcellation method employed. The time series of each voxel in the VOI was extracted and their pairwise similarity calculated to construct a similarity matrix per run per participant. Each matrix has all the VOI voxels as rows and all the same VOI voxels as columns. The similarity matrix from each run of each participant was averaged (using z-score normalised correlation values) to get a group similarity matrix. This group similarity matrix was spectrally reordered resulting in voxels with a more similar time series being placed closer together on the axes. The voxel order on the axes can then be projected on to the cortex to show the graded change in connectivity across the cortex. The rank order of the voxels in the reordered matrix is projected as a value to each corresponding voxel (e.g., the 1st voxel in the reordered matrix is given the value 1) and this ordering represented by a colour spectrum (from the voxel with value 1 shown in purple to the final voxel with a value equal to the number of voxels in the VOI shown in red). Hard clusters were also identified in the reordered matrix. These clusters are areas with distinct connectivity. The voxels forming these clusters can also be shown on the cortex.

in the same manner as the previous report (Jackson et al., 2016). This included the use of four methods shown to greatly reduce the effects of motion: censoring; global signal regression; 24 motion parameter regression; and scrubbing of high motion time points identified using the ARtifact detection Tools software package (ART; www.nitrc.org/projects/artifact_detect). These methods are in keeping with other resting-state studies and were shown not to relate to the seed-based functional connectivity results reported previously, suggesting a

successful removal of motion artefact (Weissenbacher et al., 2009; Anderson et al., 2011; Power et al., 2014; Yan et al., 2013; Van Dijk et al., 2012; Power et al., 2015; Jackson et al., 2016).

Statistical parametric mapping (SPM 8) software (Wellcome Trust Centre for Neuroimaging) was used for slice timing correction, realignment and coregistration to the individual's structural image. Nuisance covariate regression was performed in the Data Processing Assistant for Resting State fMRI (DPARSF Advanced Edition, V2.3)

toolbox (Chao-Gan and Yu-Feng, 2010) and the images were normalised using DARTEL (Ashburner, 2007) and smoothed with an 8 mm full-width half maximum (FWHM) Gaussian kernel. The results were filtered at .01–.08 Hz (Satterthwaite et al., 2013). Six participants were excluded from the analysis due to having more than 3 mm translation or 1 degree of rotation or with less than 5 min of data remaining after scrubbing high motion time points. The preprocessing is described in more detail in the prior seed-based functional connectivity paper (Jackson et al., 2016).

As the effects of motion are still critical and could affect the functional parcellation results, the active task data were processed in a similar way to the resting-state data. This resulted in the exclusion of one high motion participant (leaving 23 participant's datasets). However, two steps were excluded from the process as it was considered they may affect the relation between areas related to the task. The global tissue signal value was not used as a covariate as it may change the overall task relations. Additionally, the frequency filter was not applied. The filter is designed to limit the resting-state data to include high frequency fluctuations between resting-state networks (Power et al., 2014). This would remove the lower frequency fluctuations related to the task model and therefore important functional variation would be excluded from the task data. Although not performing these steps mean less motion artefact may be removed than in the resting-state data, the task data are still heavily cleaned compared to standard task preprocessing.

Functional parcellation analyses

The functional parcellation scheme is based on a spectral reordering method first proposed for tractography data (Bajada et al., in press; Johansen-Berg et al., 2004). This method employs a graph theoretical approach and has roots in other clustering methods, particularly normalised cut clustering (von Luxburg, 2007; Shi and Malik, 2000). However, whereas normalised cut clustering leads to a series of hierarchical discrete regions the present technique is focussed on identifying the graded changes across an area. A volume of interest (VOI) was created to delineate the area to be parcellated. The probabilistic MNI temporal lobe VOI available in FSL was binarised at a certainty of 0.25 and split in to left and right temporal lobes. The resulting binary left and right temporal lobe VOIs were resliced in SPM to match the functional data. Four separate parcellations were performed; parcellation of the left and right temporal lobes employing resting-state and task data. This analysis was performed in Matlab using a GUI toolbox created and is freely available online (Functional Parcenip; see Supplementary materials).

Existing functional parcellation methods may be difficult to reproduce and direct comparison shows little benefit of one method over another (Thirion et al., 2014). Here a spectral reordering method was employed. One key reason for reordering rather than purely a hard cluster approach was to gain maps of the graded change in the relation to different clusters across the cortex. This allows identification of the critical axis of change across the temporal lobe. There may be artefactual causes of some small local gradations in functional data as the voxels are not independent due to smoothing, interpolation and motion artefacts (Power et al., 2014; Van Dijk et al., 2012; Yan et al., 2013; Friston et al., 1996). Most importantly, the convergence of modality-specific regions and the transition to modality-general regions is expected to be graded (Braga et al., 2017). Therefore, visualising the full gradient using spectral re-ordering is necessary and it may be suboptimal to force intermediate regions in to a hard cluster. In addition, identifying core regions where connectivity is highly similar (i.e., approximating distinct hard clusters) is critical for interpreting the parcellation and the function of these regions. The spectral re-ordering method can provide both a map of the graded change in functional connectivity and hard clusters, and thus was considered ideal for the targets of this investigation.

Fig. 1 presents a visual description of the pipeline. All processing was performed in MNI space to allow simple transition between individuals and the group. Firstly, the time series of every voxel in our region of interest (the temporal lobe) was extracted using an in-house MATLAB script. Secondly, the time series of each voxel was compared to the time series of every other voxel using the cosine similarity metric. This resulted in an unordered similarity matrix per individual (for the resting state parcellation) or per each run of each individual (for the task parcellation). The average of these matrices was computed (averaging the similarity across runs and participants) resulting in a single group similarity matrix (per parcellation). As correlation values are not normally distributed and can only fall within a specific interval (−1 to 1) averaging can result in bias. To avoid this, the values were z-transformed prior to averaging and then transformed back to their original values after obtaining the group result (Dunlap et al., 1983). The group matrices were then spectrally reordered using the algorithm laid out in Johansen-Berg et al. (2004). The algorithm treated the matrix as a graph's adjacency matrix and its Laplacian was calculated. The Laplacian was spectrally decomposed into its eigenvectors and corresponding eigenvalues. The second smallest (Fiedler) vector was identified and the original matrix is reordered according to the permutation vector obtained by sorting the Fiedler vector. This forces entries that have high similarity close to each other on the diagonal (Devlin et al., 2006). The resulting reordered matrix still consists of all of the voxels in both the rows and the columns. After the reordering step, those voxels that have the most similar connectivity are shown closest to each other.

Finally, the reordered voxels were projected back onto the cortex. This was done in two ways. Firstly, the order of the voxels in the reordered similarity matrix provides information on the time series; nearby voxels have the most similar time series and those furthest away have the most distinct connectivity. Therefore by showing the position of each voxel in the reordered matrix we can visualise the overall pattern of connectivity change across our VOI. Each voxel is given a value reflecting its position on the reordered matrix, e.g. the first voxel will be given the value 1. These numbers are associated with a colour spectrum from purple to red. Therefore the voxels on the left of the reordered matrix are purple and voxels slightly further right are blue, and so on until the final voxels are red. This spectrum shows the gradient of similarity across the VOI, with more similar colours having a more similar time series (i.e., two red voxels have a very similar time series that is very different to a purple voxel). This approach allowed visualisation of the general pattern of similarity across the VOI. The resulting reordered matrix is equivalent to its reverse, therefore gradients showing the same pattern of results as the other parcellation results but going in the opposite direction were inverted for display purposes (i.e. all the gradations are shown as going from posterior temporal to anterior temporal regions as opposed to anterior to posterior regions). As the order of the voxels is determined based on the Fiedler vector, the actual values of the Fiedler vector could be projected to each voxel instead of the rank order of the voxels on this vector. This would show an identical pattern of connectivity changes but instead of showing each voxel as equally different to its nearest neighbour it would allow different magnitudes of difference to be reflected (closer numbers would reflect more similar time series). However, these differences would depend on the variance in the data and may be highly susceptible to outliers. As the magnitude of differences may be misleading, only the rank order is presented in the main text but information on the magnitude of the Fiedler vector is available in Supplementary Fig. 2. The second approach was to identify hard clusters as in previous studies (Johansen-Berg et al., 2004; Devlin et al., 2006). These hard clusters show areas of distinct connectivity allowing further interpretation of the connectivity differences underlying the graded result. Areas showing high similarity (i.e., strong correlation between these voxels and low correlation with other clusters) were determined through visual inspection of the matrix.

These areas of similar connectivity can be projected to the brain by binary inclusion of voxels in this area of the matrix only. The hard clusters were determined by eye following prior investigations of structural connectivity (Johansen-Berg et al., 2004; Devlin et al., 2006) in order to maintain a data-driven approach that does not force the data to fit any *a priori* constraints (such as the number or size of clusters). This allows the closest approximation of the true areas with distinct connectivity and therefore the closest approximation of possible functional subregions and the distinct functional connectivity patterns underlying the connectivity gradient. In order to demonstrate that the connectivity differences were not related to the inclusion of a different number of voxels in each hard cluster, clusters were also extracted using a percentile-based threshold (see Supplementary materials).

Functional connectivity and co-activation analyses

The functional parcellation of the resting-state and task-state data was based on the similarity between the voxels time series. The hard clusters arising from this parcellation have distinct time series. Their involvement in different networks outside of the temporal lobe can therefore be investigated to aid interpretation of why they were separated in the data-driven parcellation. The functional connectivity of these regions outside the temporal lobe was determined using seed-based functional connectivity analyses across the whole brain in DPARSF (Yan et al., 2013; Chao-Gan and Yu-Feng, 2010). The resting-state connectivity of the clusters identified in the resting-state parcellation and the task-state connectivity of the clusters identified in the task-state parcellation were assessed. Functional connectivity maps were z-score normalised. Paired t-tests were performed on the z-score normalised functional connectivity map to identify which areas showed greater connectivity to one cluster than the other. The resulting images were thresholded at a voxel-level threshold of .001 and FWE-corrected at the cluster level with a critical cluster level of .05.

The use of simple functional connectivity measures with task data is unusual. This is because simple correlation measures cannot separate true connectivity from the co-activation of two areas based on the relation to the task model. For instance, the presentation of a stimulus may engage attention areas and visual areas without any connection between these regions (Friston, 1994). Thus, the connectivity maps derived using the task data may reflect true connectivity or co-activation. This means the resultant maps should not be over interpreted in terms of connectivity nor should they be directly compared to the resting-state connectivity maps (especially as there are also differences in VOI extent and preprocessing steps). However, the distinction between the connectivity/co-activation maps of distinct clusters can still be interpreted as suggesting differential network involvement, and thus used to aid interpretation of the functional parcellation.

VOI analyses

A further analysis was performed to investigate the function of the regions within the hard clusters by directly testing the hypothesis that the functional parcellation separated modality-specific and modality-general areas (Braga et al., 2017). The core regions of interest were identified by combining the parcellation results based on the resting-state and task data (i.e. the first cluster in the resting-state data was combined with the first cluster in the task data and the second with the second). This was done separately for the left and right results. Voxels were included if they were identified in both the resting-state and task results. The resulting combined clusters were split into areas of contiguous voxels for use as VOIs.

VOI analysis was performed on an independent data set previously reported in Rice et al. (submitted for publication). Rice et al. (submitted for publication) presented famous people, animals and famous

landmarks in the visual domain (as pictures) and the auditory domain (as spoken words). In the semantic conditions, participants made a nationality judgement and in the baseline conditions, participants made a sensory decision (scrambled picture high or low on the screen, high or low pitched scrambled tones). The previous report focussed on interpretation of the category differences. This data set was chosen to test the hypothesis that the functional parcellation separated modality-specific and modality-general areas for three reasons. Firstly, the data included a manipulation of modality which is the critical question here. As items were presented in either the visual or auditory modality and then processed semantically, divisions between auditory-only, visual-only and multi-modal semantic regions could be identified. Secondly, the data were acquired using the same dual echo EPI technique used here, therefore signal was maintained in the critical inferior temporal problem regions. Thirdly, this data set is independent of both the resting-state and task-state parcellations and therefore any statistical circularity is avoided. The data were processed in a standard fashion (see Rice et al., submitted for publication). Standard VOI analyses were performed in the MarsBar toolbox (Brett et al., 2002) to extract the beta values for the auditory and visual conditions. The extent to which each VOI was modality-specific or modality-general was then directly tested by contrasting the auditory and visual values using paired t-tests. The average modality difference (visual contrast value − auditory contrast value) per VOI was plotted for display purposes.

Secondary differences in functional connectivity by modality

Although the principal axis of connectivity change is proposed to be the modality-specific vs. modality-general dimension, the specific modality (e.g., visual vs. auditory) may relate to secondary connectivity differences. The modality-specific VOIs were therefore split in to visual and auditory regions on the basis of the VOI analysis and their resting-state functional connectivity determined to explore which of the regions connected to the modality-specific cluster are connected similarly to both VOIs and which are differentially connected. In order to fully clarify both the similarities and differences within the modality-specific network, both within and between t-tests were employed, masked by the resting-state connectivity map of the entire modality-specific cluster.

Results

Resting-state functional parcellation

The group-level results of the resting-state parcellation of the left and right temporal lobes are shown in Fig. 2. The similarity matrix of the left temporal lobe showed clear structure in the similarity of the voxels time series. The cortical projection of the graded change (see Fig. 2.B) showed a similarity between inferior posterior temporal cortex (including fusiform, inferior and middle temporal gyri) and the superior temporal gyrus (STG). The voxels most distinct to these regions were within the anterior inferior and middle temporal gyri and the temporal pole. Intermediate connectivity patterns were observed within the medial temporal lobe and intermediate areas. The similarity matrix clearly shows two distinct clusters in the left temporal lobe. The portion of the matrix included in each cluster is highlighted by the purple and red bars underneath the matrix (i.e. the first voxels up to the end of the purple bar are in the purple cluster and the last voxels from the start of the red bar are in the second cluster). These areas are shown in Fig. 2.C. The first cluster (shown in purple) included posterior fusiform gyrus (FG), inferior temporal gyrus (ITG) and middle temporal gyrus (MTG), as well as some small areas of posterior and anterior STG. The second cluster (shown in red) included the temporal pole, anterior ITG and the MTG.

The right temporal lobe showed an extremely similar gradient in connectivity from posterior inferior temporal cortex and the STG to
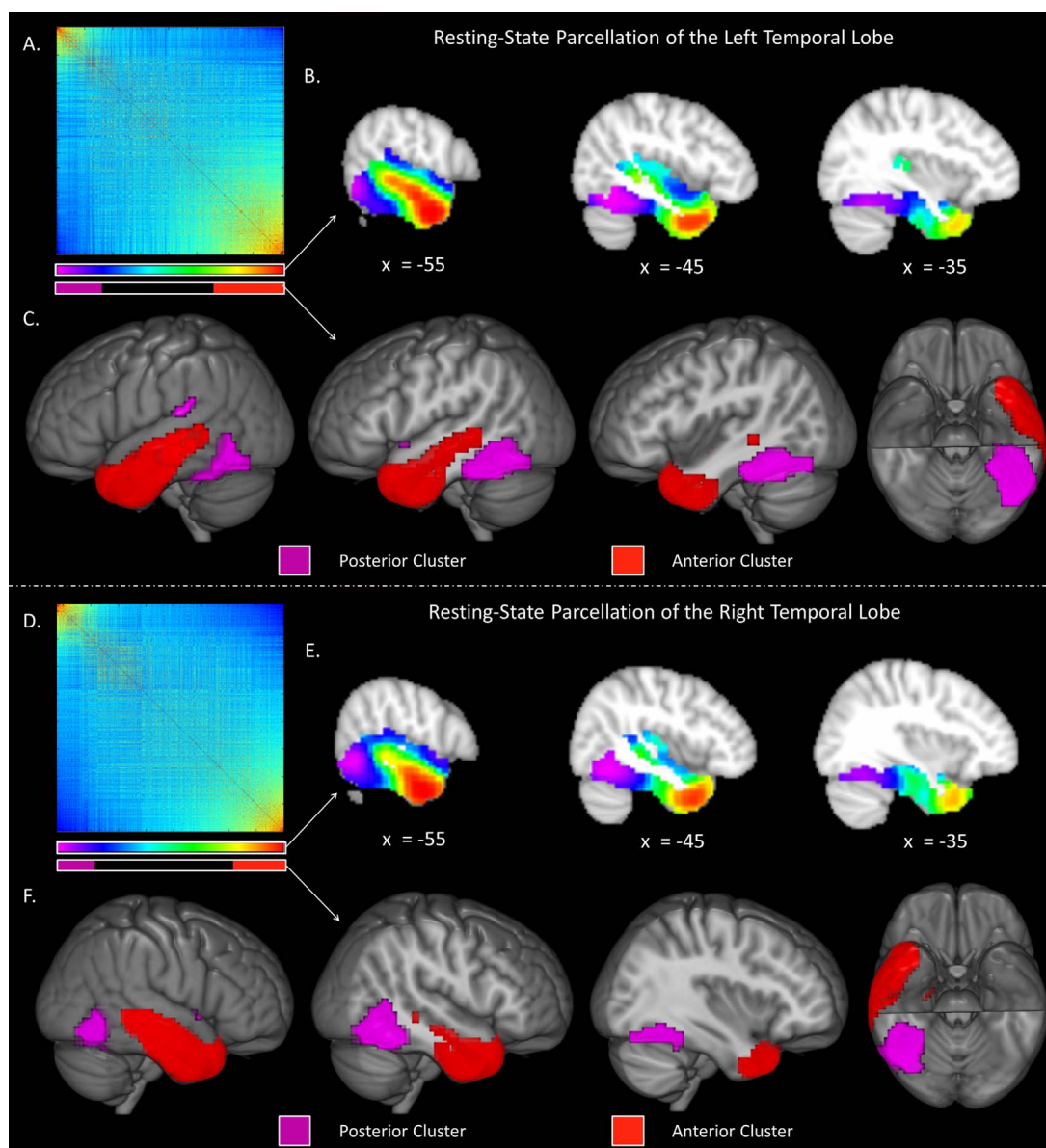
Fig. 2. The results of the functional parcellation of the left (A, B and C) and right (D, E and F) temporal lobes based on resting-state data. A & D. Matrices showing the pairwise similarity of the voxels time series, reordered so that nearer voxels are more similar. Rows and columns show all voxels in this connectivity-based order. The gradient of connectivity can therefore be seen by showing the order of the voxels on the cortex. Each row of the matrix is given a colour along a colour spectrum shown below the matrix. This order may be projected on to the cortex to show graded changes in functional connectivity (in B & E). Additionally, distinct clusters may be identified within the matrix based on its structure. The rows of the matrix included in these clusters are shown by the red and purple bars. The location of these voxels can be viewed on the cortex (in C & F). B & E. The similarity of the voxels projected on to the cortex. The colours represent similarity (e.g. red areas have the most distinct time series from purple areas). Correspondence with the rows in the matrix can be determined using the rainbow colour bar below the matrix in A. A graded change may be seen from ventrolateral and polar anterior temporal lobe to inferior posterior temporal lobe and the superior temporal gyrus. C & F. The voxels that were involved in the two clusters apparent in the matrix are shown on the cortex. A posterior cluster (purple) and an anterior cluster (red) were identified in the left and the right hemisphere. The rows of the matrix included within these clusters are highlighted in red and purple in the bar below the matrix.

inferior, middle and polar regions of the ATL. This high level of similarity was confirmed by plotting the rank position of each equivalent voxel in the reordered matrix of the left and right temporal lobes (see Supplementary Fig. 3). Voxels that did not overlap exactly between the left temporal lobe and the flipped right temporal lobe ROI (rotated 90 degrees over the x=0 axis) were excluded from this analysis. The correlation between the rank positions of the left and right voxels was highly significant (r_s=.928, p < .001). The connectivity differences across the right temporal lobe were also reflected in two distinct clusters, shown in Fig. 2F. The first (purple) cluster included posterior FG, ITG and MTG, as well as a small region of anterior STG. The second (red) cluster included temporopolar cortex, anterior ITG and MTG and a small region of the parahippocampal gyrus. Although the medial temporal lobe showed a similar intermediate pattern on the left

and right temporal lobe results, there appeared to be differentiation within the medial temporal lobe with some regions being more similar to the ATL. Some of this area formed part of the anterior cluster on the right.

Task-based functional parcellation

The group-level results of the task-based parcellation of the left and right temporal lobes are shown in Fig. 3. A greater overall similarity in the voxel time series was observed in the task-based than resting-state matrices. This may relate to differences in cleaning, a real state difference in functional connectivity, or the additional co-activation effects within the task. Structure was found in the task data similarity matrices. The graded similarity maps (Fig. 3B) of both the left and right
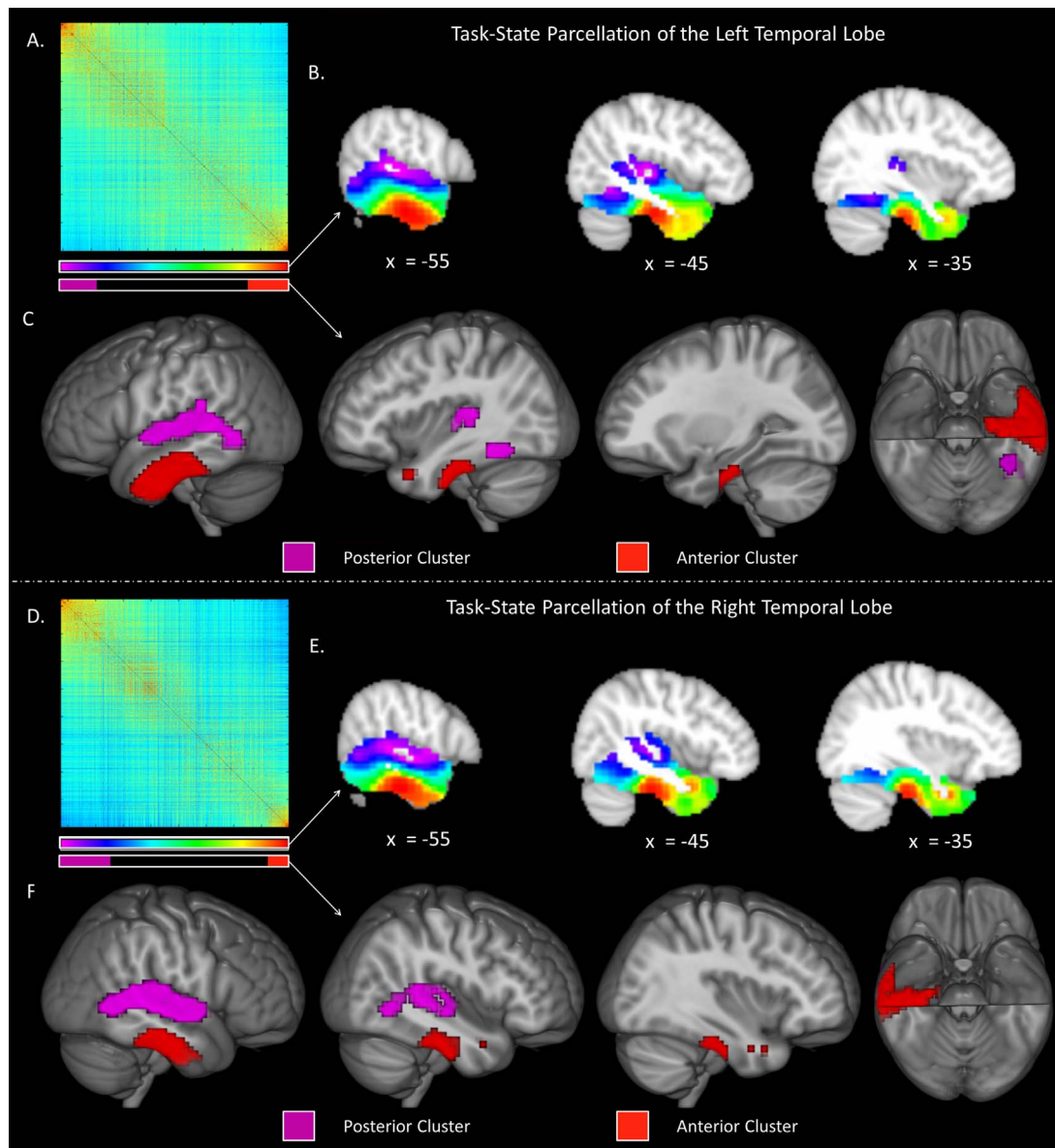
Fig. 3. The results of the functional parcellation of the left (A, B and C) and right (D, E and F) temporal lobes based on task-state data. A & D. Matrices showing the pairwise similarity of the voxels time series, reordered so that nearer voxels are more similar. Rows and columns show all voxels in this connectivity-based order. The gradient of connectivity can therefore be seen by showing the order of the voxels on the cortex. Each row of the matrix is given a colour along a colour spectrum shown below the matrix. This order may be projected on to the cortex to show graded changes in functional connectivity and co-activation (in B & E). Additionally, distinct clusters may be identified within the matrix based on its structure. The rows of the matrix included in these clusters are shown by the red and purple bars. The location of these voxels can be viewed on the cortex (in C & F). B & E. The similarity of the voxels projected on to the cortex. The colours represent similarity (e.g. red areas have the most distinct time series from purple areas). Correspondence with the rows in the matrix can be determined using the rainbow colour bar below the matrix in A. A graded change may be seen from ventrolateral and polar anterior temporal lobe to inferior posterior temporal lobe and the superior temporal gyrus. C & F. The voxels that were involved in the two clusters apparent in the matrix are shown on the cortex. A posterior cluster (purple) and an anterior cluster (red) were identified in the left and the right hemisphere. The rows of the matrix included within these clusters are highlighted in red and purple in the bar below the matrix.

temporal cortices exhibited a graded change from regions of STG and posterior MTG, ITG and FG towards the inferior ATL. A high level of similarity between left and right temporal lobes was again confirmed by plotting the rank position of each equivalent voxel in the left and right temporal lobes (r_s=.945, p < .001; see Supplementary Fig. 3). In the left hemisphere, the first (purple) cluster included Heschl's gyrus and posterior STG as well as a distinct set of voxels in posterior ITG and FG. The second cluster (shown in red) included anterior MTG, ITG, FG and parahippocampal gyrus (see Fig. 3B). In the right temporal cortex the first (purple) cluster included STG, Heschl's gyrus and posterior MTG, ITG and FG and the second cluster (shown in red) included anterior MTG, ITG, FG and parahippocampal gyrus (see Fig. 3E).

Functional parcellation results

Overall, the functional parcellation of the left and right temporal lobes using resting-state and task-state data garnered consistent results. Two distinct clusters were identified. The first was in posterior inferior temporal regions (FG, ITG and MTG) as well as STG and Heschl's gyrus, which we shall refer to as the 'posterior cluster'. The second included ventral, lateral and polar ATL (including FG, ITG, MTG and the temporal pole), which we shall refer to as the 'anterior cluster'. The results in the left and right temporal lobes were extremely similar. Some small differences were found between the resting-state and task-based parcellation results. The posterior cluster included
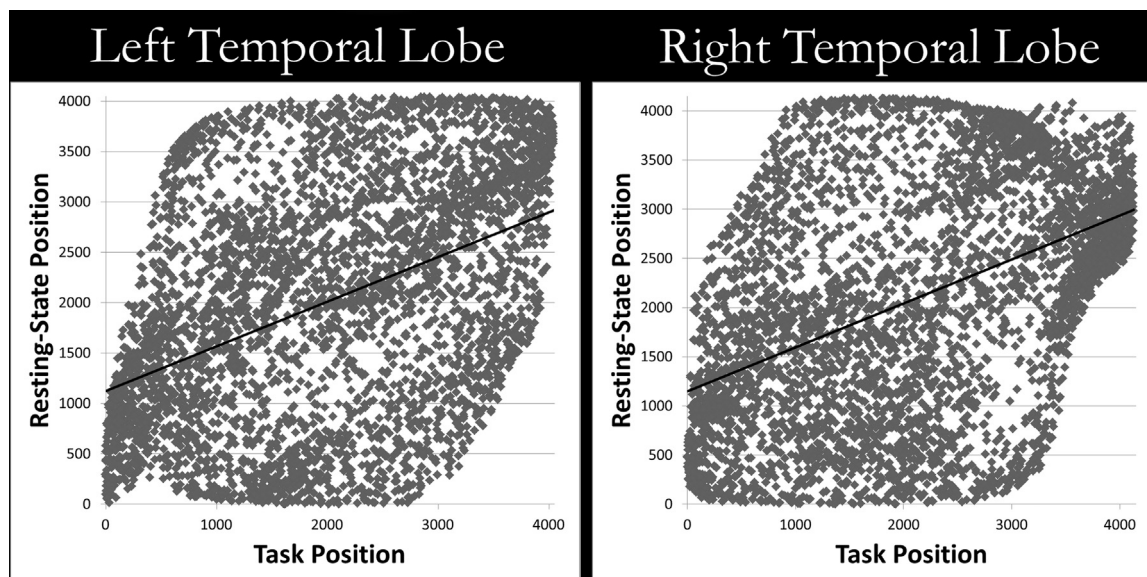
Fig. 4. The relationship between a voxels position in the graded resting-state parcellation and the graded task-state parcellation. Consistency can be seen between these two results which are shown to correlate at r_s=.449 in the left temporal lobe and r_s=.443 in the right temporal lobe.

more superior temporal cortex in the task-state results and less inferior regions. However, both results included some inferior and some superior regions and the graded similarity map showed that both regions were highly distinct from the anterior cluster. The anterior cluster was more ventral in the task-based results and more lateral, including more posterior MTG, in the resting-state based parcellation. These differences were small compared to the overall consistency in the parcellation results and might relate to real state differences in functional connectivity or the co-activation of temporal lobe regions induced by the task model. Alternatively, these small differences might reflect the unavoidable differences in pre-processing and cleaning applied to the two datasets. The consistency between the resting-state and task results can be determined by eye. Additionally we can demonstrate this consistency formally by determining the relationship between the position of each voxel in the reordered matrix based on the resting-state data and the reordered matrix based on the task-state data (see Fig. 4). The positions of the voxel in the gradient for the resting-state and task-state data (i.e., the rank order of the voxel on the Fiedler vector, corresponding to the colour spectrum in Figs. 2 and 3) were significantly correlated (left temporal lobe; r_s=.443, p < .001; right temporal lobe; r_s=.449, p < .001). As there is therefore a high level of consistency between the two results and because we cannot determine the cause of the minor differences, the rest of the paper will focus on the consistent separation of the anterior and posterior regions.

The posterior cluster included modality-specific areas (including visual and auditory areas), whereas the anterior cluster involved areas considered critical for multimodal semantic cognition. Two supporting analyses were performed to test this interpretation. First, as the parcellation identified areas with distinct functional connectivity within the temporal cortex, the functional connectivity of these clusters to areas outside of the temporal cortex was assessed. The resultant cluster-based networks should give clues as to their function. Secondly, the function of the anterior and posterior clusters was tested directly using a VOI analysis of independent task data.

Functional connectivity of the anterior and posterior clusters to regions outside the temporal lobe

The difference in resting-state functional connectivity for the anterior (anterior > posterior) and posterior (posterior > anterior) clusters is shown in Fig. 5.A (for details see Tables 1 and 2). Voxels shown

are significant at .001 with an FWE-correction at the cluster level with a critical cluster level of .05. The left posterior cluster was connected throughout bilateral occipital lobe and in superior and inferior parietal cortex and supramarginal gyrus. Connectivity was observed throughout inferior, middle and superior frontal gyri and in the somatosensory and motor cortices as well as in the insula, thalamus and cerebellum (see Table 1). The anterior cluster was connected along the MTG posteriorly in to angular gyrus (AG), dorsally to the postcentral gyrus and medially to the insula, posterior cingulate cortex and supplementary motor area. Additional connectivity was identified in the ventral inferior frontal gyrus (IFG; pars orbitalis and triangularis), middle frontal gyrus, medial prefrontal cortex and cerebellum (see Table 1). The connectivity of the anterior and posterior clusters in the right hemisphere was strikingly similar and all of the same regions were identified.

The connectivity of the anterior and posterior clusters identified using the task data was also assessed. The results are shown in Fig. 5B. Voxels shown are significant at .001 with an FWE-correction at the cluster level with a critical cluster level of .05. The task-based connectivity of the anterior cluster was similar to that observed in the resting-state data. The results for the anterior cluster in the left temporal cortex included ventral (IFG, orbitofrontal cortex, ventral medial prefrontal cortex) and dorsal regions of lateral and medial frontal cortex (dorsal medial prefrontal cortex and middle frontal gyrus), as well as bilateral AG, posterior cingulate cortex, precuneus and cerebellum (see Table 2). The right temporal anterior cluster results included similar regions but lacked significant voxels within the precuneus. In keeping with the resting-state connectivity results, the left posterior cluster analysis identified significant clusters throughout occipital cortex, superior parietal cortex, supramarginal gyrus, lateral frontal, motor cortex, insula, thalamus and cerebellum. Additional significant areas included supplementary motor area, postcentral gyrus, precuneus and anterior and mid regions of the cingulate cortex. The same areas were identified with the right posterior cluster (see Table 2). The distinct connectivity of the anterior and posterior clusters was not merely due to differences in the number of voxels included in the two clusters. In order to demonstrate this, two equally-sized hard clusters were extracted by taking the first and last 15 percent of the voxels from the reordered matrix. These regions showed distinct connectivity in the same regions as the full anterior and posterior clusters (see Supplementary Figs. 4 and 5).

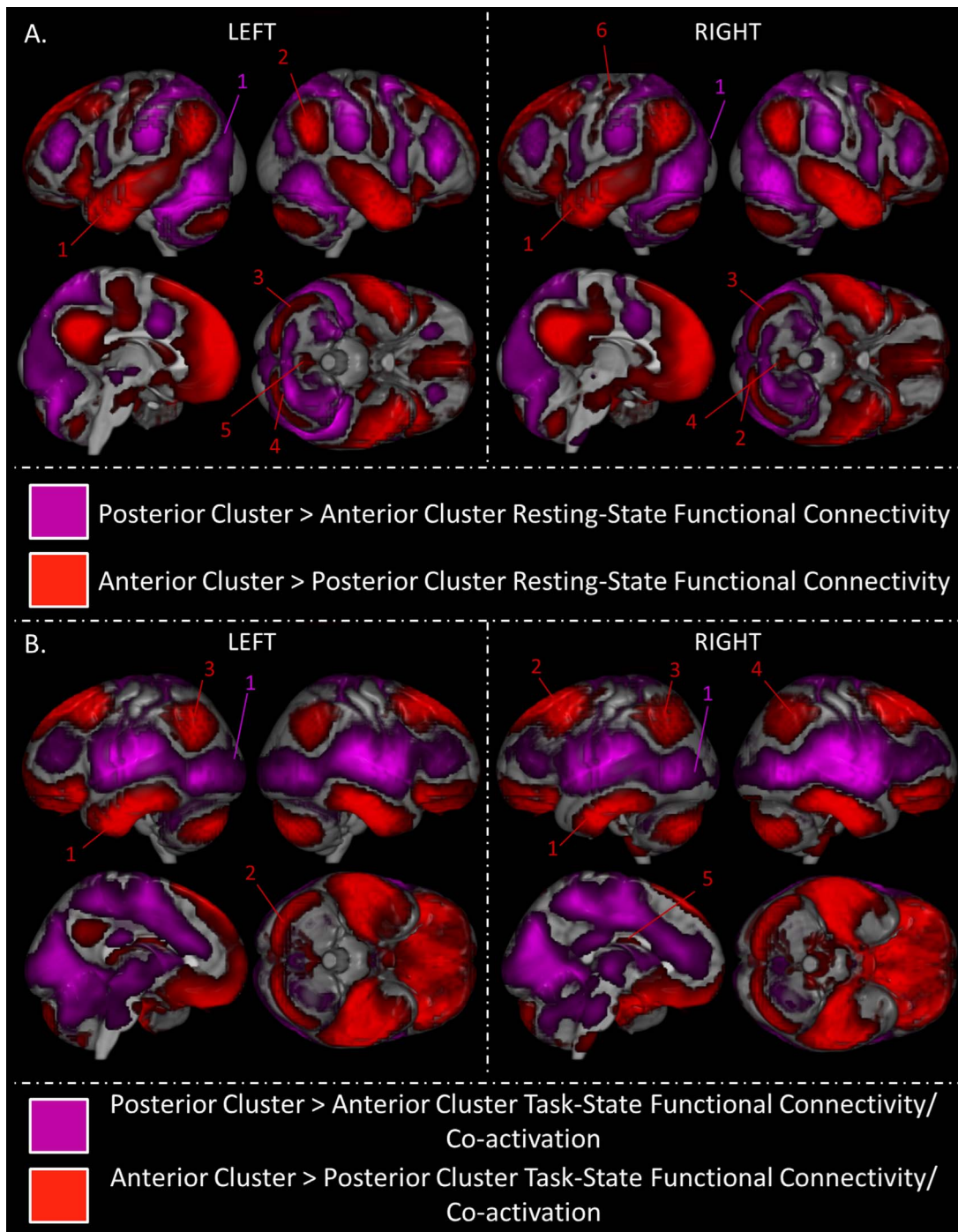Overall, similar connectivity was identified in the resting-state and

Fig. 5. Connectivity and co-activation of the clusters identified within the resting-state and active task data. A. Areas displaying greater resting-state functional connectivity with the first more posterior cluster (purple) and the second more anterior cluster (red). This analysis was performed using the clusters identified in the resting-state parcellation of the left and right temporal lobes. Each set of contiguous voxels is labelled in order to aid understanding of the correspondence with the Results section. See Table 1 for anatomical descriptions of each cluster. B. Areas displaying greater functional connectivity and co-activation in the task data with the first more posterior cluster (purple) and the second more anterior cluster (red). This analysis was performed using the clusters identified in the task-based parcellation of the left and right temporal lobes. Each set of contiguous voxels is labelled in order to aid understanding of the correspondence with the Results section, except cluster 5 which is subcortical and cannot be seen in these views. See Table 2 for anatomical descriptions of each cluster. Voxels significant at .001 with an FWE correction at the cluster level with a critical cluster level of .05.

task-based analyses. The anterior clusters connected to AG, IFG, medial prefrontal cortex and posterior cingulate cortex. The posterior clusters connected to occipital, superior parietal, supramarginal gyrus and postcentral gyrus. These results are consistent with the involvement of the anterior cluster in modality-general networks and the posterior cluster in modality-specific networks (see Discussion).

VOI analysis of modality effects within the anterior and posterior clusters

Paired t-tests were performed to compare the beta values of the visual and auditory semantic cognition conditions (i.e., a semantic decision on stimuli presented as a picture vs. a spoken word) for each

Table 1

Comparing the functional connectivity of the resting-state clusters.

Contrast	Region of activation	Cluster extent (voxels)	Max z value	P value (FWE corrected)	Peak MNI coordinate		
					X	Y	Z
Left temporal lobe posterior cluster > Anterior cluster	Bilateral posterior temporal, STG, occipital, precuneus, superior & inferior parietal, SMG, motor, somatosensory cortex, SMA, lateral frontal, thalamus, insula & cerebellum	23,600	Inf	> .001	−51	−63	−12
Left temporal lobe anterior cluster > Posterior cluster	Bilateral ATL, posterior MTG, IFG, insula, post CG, mPFC, MFG, PCC, SMA & left AG	17,397	Inf	> .001	−51	0	−36
	Right AG	597	Inf	> .001	57	−63	33
	Right cerebellum	513	Inf	> .001	24	−84	−36
	Left cerebellum	279	Inf	> .001	−30	−84	−39
	Bilateral cerebellum	238	7.15	> .001	9	−54	−42
Right temporal lobe posterior cluster > Anterior cluster	Bilateral posterior temporal, STG, occipital, precuneus, superior parietal, SMG, motor, lateral frontal, thalamus, insula & cerebellum	23,079	Inf	> .001	48	−60	−15
Right temporal lobe anterior cluster > Posterior cluster	Bilateral ATL, posterior MTG, IFG, mPFC, MFG, PCC, SMA, AG, right insula & left post CG	18,520	Inf	> .001	51	3	−36
	Left cerebellum	410	Inf	> .001	−27	−81	−36
	Right cerebellum	571	Inf	> .001	24	−84	−36
	Bilateral cerebellum	292	Inf	> .001	−6	−57	−45
	Left insula	552	6.21	> .001	−36	−21	18
	Right post CG	96	5.28	.034	27	−27	60

Clusters significant at .05 after FWE correction. MTG=middle temporal gyrus, STG=superior temporal gyrus, ATL=anterior temporal lobe, IFG=inferior frontal gyrus, mPFC=medial prefrontal cortex, MFG=middle frontal gyrus, SMA=supplementary motor area, PCC=posterior cingulate cortex, CG=central gyrus, SMG=supramarginal gyrus and AG=angular gyrus.

area in the anterior and posterior clusters. The modality difference is shown in Fig. 6. All results are shown after application of a Bonferroni correction for multiple comparisons based on the use of nine VOIs. None of the anterior VOIs showed a significant difference between the visual and auditory semantic conditions (A1; t(19)=−1.737, p > .5; A2; t(19)=−0.457, p > .5; A3; t(19)=−1.684, p > .5; A4; t(19)=−2.133, p > .1). In contrast, all of the posterior VOIs showed a significant difference between the visual and auditory semantic conditions. The three posterior VOIs located within the STG showed significantly more activation for the auditory semantics condition (P1; t(19)=−9.153, p < .001; P2; t(19)=−10.442, p < .001; P3; t(19)=−7.756, p < .001). The two posterior VOIs in the inferior posterior temporal cortex showed significantly more activation for the visual semantics condition (P4; t(19)=10.583, p < .001; P5; t(19)=4.681, p < .005). (Fig. 7).

Secondary differences in functional connectivity by modality

The posterior cluster consisted of modality-specific regions with distinct connectivity from the modality-general regions in the anterior cluster. However, the VOI analysis highlighted that some of these posterior regions are auditory (P1, P2, P3) and some are visual (P4, P5). There may be secondary differences in connectivity between these auditory and visual regions in the posterior cluster. To explore this, a single auditory VOI was created by combining P1, P2 and P3 and a single visual VOI by combining P4 and P5 (see Fig. 5). These two VOIs were used as seeds in a further seed-based functional connectivity analysis of the resting-state. Within t-tests masked by the left posterior cluster resting-state connectivity map were performed to identify which of the areas connected to the posterior cluster were connected to the auditory VOI and which to the visual VOI. The results are shown overlaid in Fig. 6B. to highlight both shared and distinct connectivity of the auditory and visual VOIs. The peak results are displayed in Table 3

Table 2

Comparing the functional connectivity and co-activation of the task-based clusters.

Contrast	Region of activation	Cluster extent (voxels)	Max z value	P value (FWE corrected)	Peak MNI coordinate		
					X	Y	Z
Left temporal lobe posterior cluster > Anterior cluster	Bilateral posterior temporal, STG, occipital, superior parietal, SMG, motor, lateral frontal, SMA, post CG, precuneus, mid & ACC, thalamus, insula & cerebellum	38,832	Inf	> .001	−63	−18	9
Left temporal lobe anterior cluster > Posterior cluster	Bilateral inferior ATL, ventral IFG, OFC, MFG, ventral & dorsal mPFC	9120	Inf	> .001	−63	−15	−27
	Bilateral cerebellum	1159	Inf	> .001	−39	−81	−42
	Bilateral AG, PCC, precuneus	2186	Inf	> .001	−45	−66	45
Right temporal lobe posterior cluster > Anterior cluster	Bilateral posterior temporal, STG, occipital, superior parietal, SMG, motor, lateral frontal, SMA, post CG, precuneus, mid & ACC, thalamus, insula & cerebellum	43,968	Inf	> .001	51	−30	6
Right temporal lobe anterior cluster > Posterior cluster	Bilateral inferior ATL, ventral IFG, OFC, ventral mPFC	7718	Inf	> .001	63	−15	−27
	Bilateral MFG & dorsal mPFC	1433	Inf	> .001	21	39	54
	Left AG	618	Inf	> .001	−51	−57	51
	Right AG	596	Inf	> .001	48	−54	57
	Bilateral PCC	408	7.16	> .001	−15	−15	27

Clusters significant at .05 after FWE correction. STG=superior temporal gyrus, ATL=anterior temporal lobe, IFG=inferior frontal gyrus, mPFC=medial prefrontal cortex, MFG=middle frontal gyrus, OFC=orbitofrontal cortex, SMA=supplementary motor area, PCC=posterior cingulate cortex, ACC=anterior cingulate cortex, CG=central gyrus, SMG=supramarginal gyrus and AG=angular gyrus.
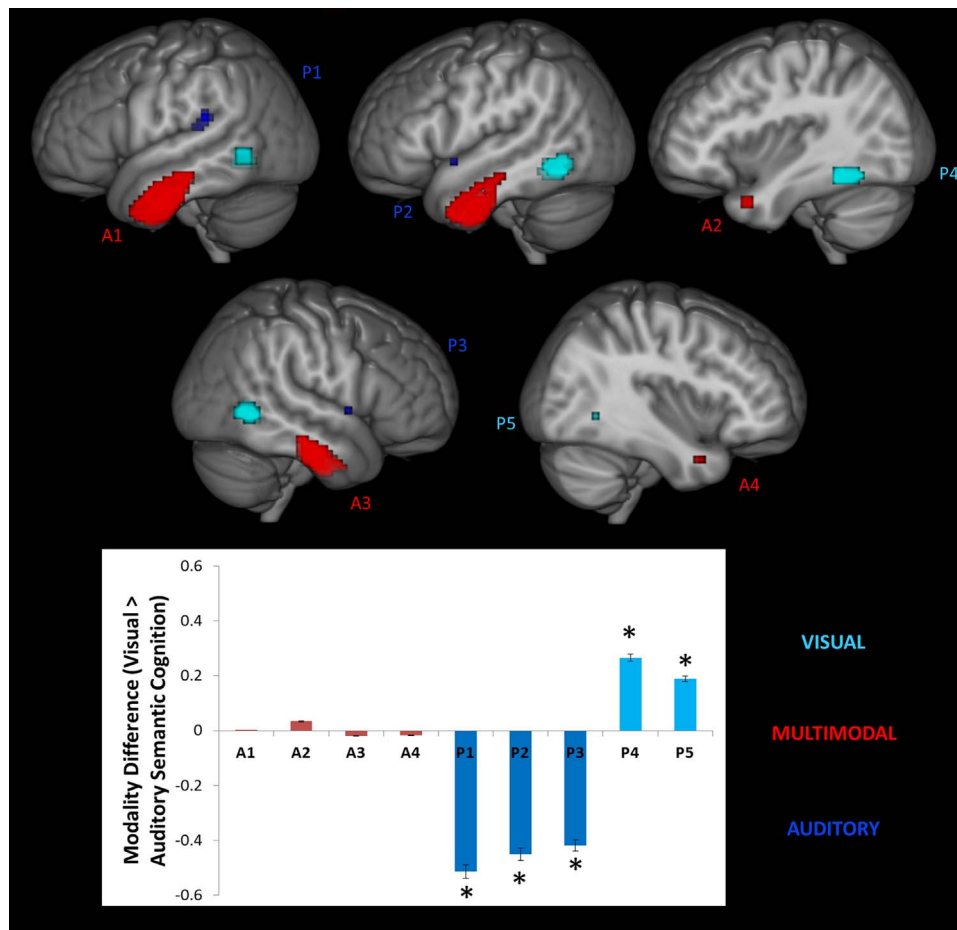
Fig. 6. A functional 'fingerprint' of the areas identified in the functional parcellations. Voxels identified as part of the anterior or posterior clusters in both the resting-state and task-based parcellations are shown here. Sets of contiguous voxels were treated separately and subjected to VOI analyses in independent functional data. The average of difference between each participant's visual and auditory beta values for each VOI are plotted here. Where the values are significantly different between the two modalities (p > .05, Bonferroni corrected) an asterisk is shown. No anterior areas showed a modality difference and can be considered multimodal (shown in red). All posterior areas showed modality differences, but those in the STG showed a preference for the auditory condition (shown in dark blue) whereas inferior regions showed a preference for the visual condition (shown in cyan). Thus, the posterior regions identified in the parcellation may be seen as modality-specific.

alongside a between t-test directly comparing the auditory and visual regions to formally identify differentially connected regions.

Both the visual and auditory regions are functionally connected to most areas identified as connected to the posterior cluster yet relative differences in involvement can be seen. The visual regions show significantly greater functional connectivity to regions within bilateral ventral occipitotemporal cortex, occipital cortex, superior and inferior parietal lobes, precuneus and cerebellum as well as the right hippocampus (see Table 3). The auditory regions show greater connectivity to bilateral posterior and anterior regions of the superior temporal gyri, supramarginal gyrus, motor cortex, superior parietal lobe, posterior and mid cingulate cortex, precuneus, insula and supplementary motor area, as well as left somatosensory cortex and right thalamus (see Table 3). These differences reflect stronger connectivity between visual regions and visual networks and between auditory regions and auditory and motor networks (see Discussion).

Discussion

A data-driven assessment of the graded change in connectivity across the temporal lobe identified the predicted critical organisational axis: from superior and posterior inferior temporal cortex to ventrolateral ATL. Consistent results were obtained across resting-state and active task data and in the left and right hemispheres. Hard parcellation identified distinct anterior (encompassing ventral, polar and lateral ATL as well as some

parahippocampal gyrus) and posterior clusters (including posterior fusiform, inferior and middle temporal gyrus as well as areas along the length of the STG). The posterior cluster connected to a wide range of regions in occipital, superior parietal, motor, anterior cingulate and lateral frontal cortex as well as supramarginal gyrus, supplementary motor area, insula, thalamus and cerebellum. The anterior cluster connected to AG, posterior cingulate cortex, precuneus, medial prefrontal cortex, ventral inferior frontal gyrus and regions of the insula and cerebellum. Thus, the parcellation identified areas consistent with the hypothesis of multimodal and modality-specific regions both within and outside of the temporal cortex. The areas identified in the posterior cluster correspond to the auditory stream along STG and the visual stream in posterior inferior temporal cortex (Felleman and Van Essen, 1991; Rauschecker and Scott, 2009). The anterior cluster (ventrolateral ATL region) is critical for multimodal semantic cognition (Binney et al., 2010; Visser et al., 2012; Visser and Lambon Ralph, 2011; Mion et al., 2010; Chen et al., 2016; Shimotake et al., 2014). This cluster includes a small portion of parahippocampal gyrus, also argued to have multimodal subregions (Mesulam, 1998). A direct test of this hypothesis showed the anterior cluster included multimodal regions only, whereas the posterior cluster included superior areas with a greater response for auditory stimuli and posterior inferior regions with a greater response for visual stimuli. Secondary differences in connectivity could be identified between those modality-specific regions associated with the auditory domain and the visual domain. This is the first formal demonstration that there is a direct
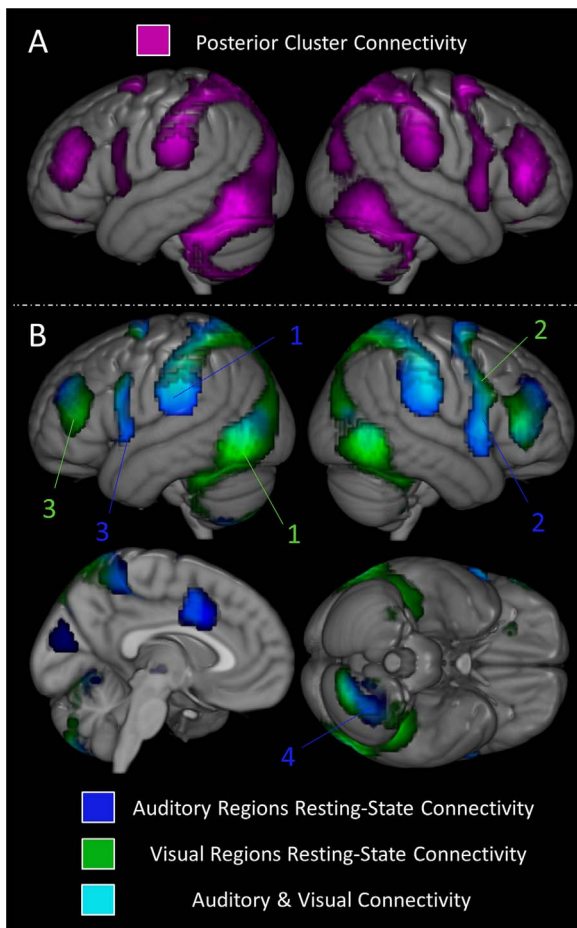
Fig. 7. The differential resting-state functional connectivity of the auditory and visual regions of the posterior cluster. A. Resting-state connectivity of the left posterior cluster as displayed in Fig. 4. B. Resting-state connectivity of the auditory regions of the posterior cluster is shown in green. Resting-state connectivity of the visual regions of the posterior cluster is shown in blue. Regions connected to both auditory and visual regions are shown in cyan. Each set of contiguous voxels is labelled in order to aid understanding of the correspondence with the Results section. See Table 3 for anatomical descriptions of each cluster. Voxels significant at .001 with an FWE correction at the cluster level with a critical cluster level of .05.

relationship between the function of the multimodal and modality-specific regions of temporal cortex and their contrastive patterns of connectivity, all revealed through a data-driven graded parcellation.

Modality-specific and modality-general regions outside of the temporal cortex

The extra-temporal areas functionally connected to the anterior and posterior clusters may reflect a similar division between modality-specific and modality-general regions. The posterior cluster connected to regions responsible for visual, auditory, somatosensory and motor processing. The functional significance of these regions is highlighted by the relative differences in connectivity between the visual regions (in ventral posterior temporal cortex) and the auditory regions (in the superior temporal gyrus) of the posterior cluster. The visual region showed relatively greater connectivity to regions within primary and association visual regions, as well as more extensive networks associated with visual processing. Occipital cortex includes primary visual and visual association cortices. In addition to the ventral visual stream, going from occipital to temporal cortex, a dorsal visual stream projects to the superior parietal lobule, connected to frontal eye fields and premotor cortex (Kravitz et al., 2011; Rozzi et al., 2006; Ungerleider and Haxby, 1994). These regions are considered critical for the

visuospatial processing necessary for object interaction (including the control of eye movements) and their functional connections constitute the dorsal attention network (Fox et al., 2006; Vossel et al., 2014; Kravitz et al., 2011). In conjunction with the ventral attention network, involving temporoparietal regions and lateral frontal cortex (inferior and middle frontal gyri), the dorsal attention network controls attentional processes related to visual stimuli (Fox et al., 2006; Vossel et al., 2014). The early and associative visual regions and the visual and dorsal attention network regions are functionally connected to the posterior cluster and show relatively greater connectivity to the visual regions of the posterior cluster.

The posterior cluster also included modality-specific auditory, motor and somatosensory regions, all showing relatively greater connectivity to the auditory regions of the posterior cluster. This included anterior and posterior superior temporal gyrus, primary and supplementary motor areas and somatosensory cortex, as well as the inferior frontal and supramarginal gyri. All of these regions have been shown to be functionally connected and have previously been considered to form a single network (Jackson et al., 2016; Beckmann et al., 2005; Smith et al., 2009; Damoiseaux et al., 2006; Xiang et al., 2010; Saur et al., 2010). The functional significance of a network composed of auditory, motor and somatosensory regions has been considered to relate to speech processing, perhaps particularly phonology or language production (Jackson et al., 2016; Xiang et al., 2010; Saur et al., 2010). Therefore, the posterior cluster connected to regions associated with modality-specific processing in the visual, auditory and motor domains reflecting multiple well-known networks (including early visual, auditory-motor, visual attention and dorsal attention networks). Both auditory and visual subregions of the posterior cluster showed strong connectivity throughout this network, with relative differences based on modality appearing subtle in comparison.

The anterior cluster connected to areas forming multimodal networks, including the semantic and default mode networks. The default mode network includes medial prefrontal and posterior cingulate cortices, precuneus, medial temporal lobe and AG (Buckner et al., 2008; Greicius et al., 2003). Although the role of the default mode network is highly contested, the hypothesised functions typically reflect multimodal processing (e.g., internally-directed attention, social cognition, episodic memory, mind wandering; Mantini and Vanduffel, 2013; Buckner et al., 2008; Andrews-Hanna et al., 2010a). Past studies have noted that the default mode network may not be a single homogeneous, stable entity. Instead, various studies have shown that the DMN is a variable patchwork of regions reflecting the fact that different areas deactivate to some but not all of the same tasks and processes (Spreng, 2012; Humphreys et al., 2015; Andrews-Hanna et al., 2010b; Jackson et al., submitted for publication; Buckner et al., 2008). However, these networks are all likely to reflect modality-general processes as they show deactivation during presentation of stimuli in different modalities. One such network includes the ventrolateral ATL, ventral inferior frontal gyrus, posterior middle temporal gyrus, ventral and dorsal medial prefrontal cortices, all of which are involved in multimodal semantic cognition (Lambon Ralph, 2014; Jefferies, 2013; Lambon Ralph et al., 2017). These regions are functionally connected during semantic processing, both in the resting-state and explicit semantic tasks, constituting a semantic network distinct from the core default mode network (Humphreys et al., 2015; Jackson et al., submitted for publication, 2016). The areas typically deactivated in the resting-state likely reflect several distinct networks yet their distinct topographies and functions remain to be elucidated (Spreng, 2012; Humphreys et al., 2015; Andrews-Hanna et al., 2010b; Buckner et al., 2008).

As the ventrolateral ATL is a multimodal semantic region responsible for integrating modality-specific information it is interesting to consider these results in light of another area of functional connectivity research; the identification of hub regions based on graph theoretical metrics (van den Heuvel and Sporns, 2013). The integration of modality-specific information within the ATL may lead to high values

Table 3
Investigating the resting-state functional connectivity of the visual and auditory regions of the posterior cluster.

Contrast	Region of activation	Cluster extent (voxels)	Max z value	P value (FWE corrected)	Peak MNI coordinate		
					X	Y	Z
Visual regions	Bilateral ventral occipitotemporal cortex, occipital cortex, precuneus, SPL & cerebellum	12123	Inf	> .001	54	−57	−3
	Right motor, insula, thalamus, lateral frontal & bilateral SMA	3047	Inf	> .001	48	6	30
	Left motor, insula, thalamus & lateral frontal	1971	Inf	> .001	−45	3	24
Auditory regions	Bilateral posterior STG, SMG, somatosensory cortex, SPL, IPL, precuneus, posterior cingulate, occipital cortex & cerebellum	6074	Inf	> .001	−60	−33	18
	Right motor, insula, thalamus, IFG & bilateral SMA	3037	Inf	> .001	36	9	6
	Left motor, insula, thalamus & lateral frontal	1611	Inf	> .001	−33	9	6
	Left cerebellum	271	Inf	> .001	−33	−57	−54
Visual > Auditory regions	Bilateral ventral occipitotemporal cortex, occipital cortex, precuneus, SPL, IPL, cerebellum & right hippocampus	9152	Inf	> .001	−48	−57	−12
	Right lateral frontal cortex	711	7.23	> .001	45	6	27
	Left IFG (pars opercularis)	187	7.21	.002	−36	0	27
	Left MFG	156	7.11	.006	−24	6	51
	Left IFG (pars triangularis)	244	6.67	> .001	−45	33	15
Auditory > Visual regions	Left posterior STG, SMG & somatosensory cortex	245	Inf	> .001	−63	−33	18
	Right posterior STG & SMG	320	Inf	> .001	60	−30	18
	Right anterior STG, insula, motor cortex & thalamus	534	Inf	> .001	60	3	3
	Left anterior STG, insula & motor cortex	361	Inf	> .001	−33	6	9
	Bilateral SMA & mid cingulate cortex	525	Inf	> .001	−6	12	33
	Bilateral posterior cingulate, precuneus & SPL	422	6.57	> .001	9	−27	45
	Right MFG	115	5.42	.021	30	39	24

Clusters significant at .05 after FWE correction. SPL=superior parietal lobe, IPL=inferior parietal lobe, STG=superior temporal gyrus, IFG=inferior frontal gyrus, MFG=middle frontal gyrus, SMA=supplementary motor area and SMG=supramarginal gyrus.

in many measures of 'hubness'. However, as this integration occurs in a graded fashion over a large area of the brain, measures of the number of connections an area has may fail to identify the ATL as a hub. Sepulcre et al. (2012) adopted a stepwise functional connectivity approach that may better reflect information flow from modality-specific sensory regions to multimodal hub areas. Using this approach an ATL region strongly resembling the anterior cluster was identified as a multimodal hub in contrast to the earlier regions in the rest of the temporal lobe.

Thus, the anterior cluster connects to modality-general semantic and default mode networks, whilst the posterior cluster connects to modality-specific visual (including early visual, ventral attention network and dorsal attention networks) and auditory-motor networks. Involvement of temporal regions in these networks is highly consistent with prior assessments of the functional connectivity of the temporal lobe (Jackson et al., 2016; Simmons et al., 2010; Pascual et al., 2013; Hurley et al., 2015; Xiang et al., 2010; Saur et al., 2010) and comparisons of functional and structural connectivity (Jung et al., 2016). Although the changes in structural and functional connectivity of the temporal cortex appear predominantly graded, this is accompanied by some sharper divides, such as the distinction between the anterior STG and the rest of the ATL. This sharp division has been demonstrated using seed-based functional connectivity measures (Saur et al., 2010; Jackson et al., 2016), cytoarchitecture (Brodmann, 1909) and the underlying structural connectivity (Saur et al., 2010; Jung et al., 2016; Binney et al., 2012).

Overall, the functional connectivity of the two hard clusters resembles the distinction between anti-correlated 'task-positive' and 'task-negative' networks (e.g. Fox et al., 2005) and it may be that modality-specific and modality-general temporal cortical regions connect to the 'task-positive' and 'task-negative' networks, respectively. This makes intuitive sense as 'task-positive' typically means stimulus-induced and therefore includes modality-specific input and output regions. However, multimodal regions responsible for controlled cognition, such as the inferior frontal gyrus, should respond more when hard tasks are performed (Vincent et al., 2008). In this study, we found that ventral inferior frontal regions were identified within the multimodal network whilst dorsal regions formed part of the modality-

specific network. Past studies have shown that distinct inferior frontal regions have different roles (Devlin et al., 2003; Binkofski et al., 1999; Molnar-Szakacs et al., 2005) and differential structural and functional connectivity with the temporal lobe (Xiang et al., 2010; Binney et al., 2012; Jung et al., 2016). Neither task-negative or task-positive networks consistently show this expected pattern of activity for all tasks (Spreng, 2012; Humphreys et al., 2015; Jackson et al., submitted for publication) therefore modality-specific and modality-general processing may be an alternative conceptualisation of this critical organisational dimension.

Appendix A. Supporting information

Supplementary data associated with this article can be found in the online version at doi:10.1016/j.neuroimage.2017.04.024.

References

Abel, T.J., Rhone, A.E., Nourski, K.V., Kawasaki, H., Oya, H., Griffiths, T.D., Howard, M.A., Tranel, D., 2015. Direct physiologic evidence of a heteromodal convergence region for proper naming in human left anterior temporal lobe. J. Neurosci. 35 (4), 1513–1520.

Acosta-Cabronero, J., Patterson, K., Fryer, T.D., Hodges, J.R., Pengas, G., Williams, G., Nestor, P.J., 2011. Atrophy, hypometabolism and white matter abnormalities in semantic dementia tell a coherent story. Brain 134, 2025–2035.

Anderson, J.S., Druzgal, T.J., Lopez-Larson, M., Jeong, E.K., Desai, K., Yurgelun-Todd, D., 2011. Network anticorrelations, global regression, and phase-shifted soft tissue correction. Hum. Brain Mapp. 32 (6), 919–934. http://dx.doi.org/10.1002/hbm.21079.

Andrews-Hanna, J.R., Reidler, J.S., Huang, C., Buckner, R.L., 2010a. Evidence for the

default Network's role in spontaneous cognition. J. Neurophysiol. 104 (1), 322–335. http://dx.doi.org/10.1152/jn.00830.2009.

Andrews-Hanna, J.R., Reidler, J.S., Sepulcre, J., Poulin, R., Buckner, R.L., 2010b. Functional-anatomic fractionation of the brain's default network. Neuron 65 (4), 550–562. http://dx.doi.org/10.1016/j.neuron.2010.02.005.

Ashburner, J., 2007. A fast diffeomorphic image registration algorithm. Neuroimage 38 (1), 95–113. http://dx.doi.org/10.1016/j.neuroimage.2007.07.007.

Bajada, C.J., Jackson, R.L., Haroon, H.A., Azadbakht, H., Parker, G.J.M., Lambon Ralph, M.A., Cloutman, L., 2017. A graded tractographic parcellation of the temporal lobe. Neuroimage. http://dx.doi.org/10.1016/j.neuroimage.2017.04.016, (in press).

Beckmann, C.F., DeLuca, M., Devlin, J.T., Smith, S.M., 2005. Investigations into resting-state connectivity using independent component analysis. Philos. Trans. R. Soc. B-Biol. Sci. 360 (1457), 1001–1013. http://dx.doi.org/10.1098/rstb.2005.1634.

Bell, A.H., Hadj-Bouziane, F., Frihauf, J.B., Tootell, R.B.H., Ungerleider, L.G., 2009. Object representations in the temporal cortex of monkeys and humans as revealed by functional magnetic resonance imaging. J. Neurophysiol. 101 (2), 688–700.

Binder, J.R., Desai, R.H., Graves, W.W., Conant, L.L., 2009. Where is the semantic system? A critical review and meta-analysis of 120 functional neuroimaging studies. Cereb. Cortex 19 (12), 2767–2796. http://dx.doi.org/10.1093/cercor/bhp055.

Binkofski, F., Buccino, G., Stephan, M., Rizzolatti, G., Seitz, J., Freund, H.-J., 1999. A parieto-premotor network for object manipulation: evidence from neuroimaging. Exp. Brain Res. 128 (1), 201–213.

Binney, R.J., Embleton, K.V., Jefferies, E., Parker, G.J.M., Lambon Ralph, M.A., 2010. The ventral and inferolateral aspects of the anterior temporal lobe are crucial in semantic memory: evidence from a novel direct comparison of distortion-corrected fMRI, rTMS, and semantic dementia. Cereb. Cortex 20 (11), 2728–2738. http://dx.doi.org/10.1093/cercor/bhq019.

Binney, R.J., Parker, G.J.M., Lambon Ralph, M.A., 2012. Convergent connectivity and graded specialization in the rostral human temporal lobe as revealed by diffusion-weighted imaging probabilistic tractography. J. Cogn. Neurosci. 24 (10), 1998–2014.

Braga, R.M., Hellyer, P.J., Wise, R.J.S., Leech, R., 2017. Auditory and visual connectivity gradients in frontoparietal cortex. Hum. Brain Mapp. 38 (1), 255–270.

Brett M., Anton J., Valabregue R., Poline J., 2002. Region of interest analysis using an SPM toolbox [abstract]. Presented at In: Proceedings of the 8th International Conference on Functional Mapping of the Human Brain, June 2–6, 2002, Sendai, Japan Available on CD-ROM in NeuroImage, vol. 16, no. 2.

Brodmann, K., 1909. Vergleichende Lokalisationslehre der Grosshirnrinde (trans: garey LJ). Springer, New York.

Buckner, R.L., Andrews-Hanna, J.R., Schacter, D.L., 2008. The brain's default network – anatomy, function, and relevance to disease. Year Cogn. Neurosci. 2008 (1124), 1–38. http://dx.doi.org/10.1196/annals.1440.011.

Chao-Gan, Y., Yu-Feng, Z., 2010. DPARSF: a MATLAB toolbox for "pipeline" data analysis of resting-state fMRI. Front. Syst. Neurosci. 4. http://dx.doi.org/10.3389/fnsys.2010.00013.

Chen, Y., Shimotake, A., Matsumoto, R., Kunieda, T., Kikuchi, T., Miyamoto, S., Fukuyama, H., Takahashi, R., Ikeda, A., Lambon Ralph, M.A., 2016. The 'when' and 'where' of semantic coding in the anterior temporal lobe: temporal representational similarity analysis of electrocorticogram data. Cortex 79, 1–13.

Colombo, M., Rodman, H.R., Gross, C.G., 1996. The effects of superior temporal cortex lesions on the processing and retention of auditory information in monkeys (Cebus apella). J. Neurosci. 16, 4501–4517.

Damoiseaux, J.S., Rombouts, S., Barkhof, F., Scheltens, P., Stam, C.J., Smith, S.M., Beckmann, C.F., 2006. Consistent resting-state networks across healthy subjects. Proc. Natl. Acad. Sci. USA 103 (37), 13848–13853. http://dx.doi.org/10.1073/pnas.0601417103.

Desimone, R., 1991. Face-selective cells in the temporal cortex of monkeys. J. Cogn. Neurosci. 3, 1–8.

Devlin, J.T., Matthews, P.M., Rushworth, M.F.S., 2003. Semantic processing in the left inferior prefrontal cortex: a combined functional magnetic resonance imaging and transcranial magnetic stimulation study. J. Cogn. Neurosci. 15 (1), 71–84.

Devlin, J.T., Russell, R.P., Davis, M.H., Price, C.J., Wilson, J., Moss, H.E., Matthews, P.M., Tyler, L.K., 2000. Susceptibility-induced loss of signal: comparing PET and fMRI on a semantic task. Neuroimage 11 (6), 589–600. http://dx.doi.org/10.1006/nimg.2000.0595.

Devlin, J.T., Sillery, E.L., Hall, D.A., Hobden, P., Behrens, T.E.J., Nunes, R.G., Clare, S., Matthews, P.M., Moore, D.R., Johansen-Berg, H., 2006. Reliable identification of the auditory thalamus using multi-modal structural analyses. Neuroimage 30, 1112–1120.

Ding, S.L., Van Hoesen, G.W., Cassell, M.D., Poremba, A., 2009. Parcellation of human temporal polar cortex: a combined analysis of multiple cytoarchitectonic, chemoarchitectonic, and pathological markers. J. Comp. Neurol. 514, 595–623.

Dunlap, W.P., Jones, M.B., Bittner, A.C., 1983. Average correlations vs. correlated averages. Bull. Psychon. Soc. 21 (3), 213–216.

Felleman, D.J., Van Essen, D.C., 1991. Distributed hierarchical processing in the primate cerebral cortex. Cereb. Cortex 1, 1–47.

Fox, M.D., Corbetta, M., Snyder, A.Z., Vincent, J.L., Raichle, M.E., 2006. Spontaneous neuronal activity distinguishes human dorsal and ventral attention systems. Proc. Natl. Acad. Sci. USA 103 (26), 10046–10051.

Fox, M.D., Snyder, A.Z., Vincent, J.L., Corbetta, M., Van Essen, D.C., Raichle, M.E., 2005. The human brain is intrinsically organized into dynamic, anticorrelated functional networks. Proc. Natl. Acad. Sci. USA 102 (27), 9673–9678. http://dx.doi.org/10.1073/pnas.0504136102.

Friston, K.J., 1994. Functional and effective connectivity in neuroimaging: a synthesis. Hum. Brain Mapp. 2 (1-2), 56–78. http://dx.doi.org/10.1002/hbm.460020107.

Friston, K.J., Williams, S., Howard, R., Frackowiak, R.S.J., Turner, R., 1996. Movement-related effects in fMRI time-series. Magn. Reson. Med. 35 (3), 346–355. http://

dx.doi.org/10.1002/mrm.1910350312.

Greicius, M.D., Krasnow, B., Reiss, A.L., Menon, V., 2003. Functional connectivity in the resting brain: a network analysis of the default mode hypothesis. Proc. Natl. Acad. Sci. USA 100 (1), 253–258. http://dx.doi.org/10.1073/pnas.0135058100.

Gross, C.G., Rocha-Miranda, C.E., Bender, D.B., 1972. Visual properties of neurons in inferotemporal cortex of the macaque. J. Neurophysiol. 35, 96–111.

Halai, A., Welbourne, S., Embleton, K.V., Parkes, L., 2014. A comparison of dual-echo and spin-echo fMRI of the inferior temporal lobe. Hum. Brain Mapp. 35 (8), 4118–4128.

Halgren, E., Dale, A.M., Sereno, M.I., Tootell, R.B.H., Marinkovic, K., Rosen, B.R., 1997. Location of fMRI responses to faces anterior to retinotopic cortex. Neuroimage 5 (4 Pt 2), S150.

Humphreys, G., Hoffman, P., Visser, M., Binney, R.J., Lambon Ralph, M.A., 2015. Establishing task- and modality-dependent dissociations between the semantic and default mode networks. Proc. Natl. Acad. Sci. USA 112 (25), 7857–7862.

Hurley, R.S., Bonakdarpour, B., Wang, X., Mesulam, M.M., 2015. Asymmetric connectivity between the anterior temporal lobe and the language network. J. Cogn. Neurosci. 27 (3), 464–473.

Jackson, R., Cloutman, L., Lambon Ralph, M., 2017. A systematic approach to elucidating the cognitive signature of resting-state networks using ICA. Cereb. Cortex, (submitted for publication).

Jackson, R.L., Hoffman, P., Pobric, G., Lambon Ralph, M.A., 2015. The nature and neural correlates of semantic association vs. conceptual similarity. Cereb. Cortex.

Jackson, R.L., Hoffman, P., Pobric, G., Lambon Ralph, M.A., 2016. The semantic network at work and rest: differential connectivity of anterior temporal lobe subregions. J. Neurosci. 36 (5), 1490–1501.

Jefferies, E., 2013. The neural basis of semantic cognition: converging evidence from neuropsychology, neuroimaging and TMS. Cortex 49 (3), 611–625. http://dx.doi.org/10.1016/j.cortex.2012.10.008.

Johansen-Berg, H., Behrens, T.E.J., Robson, M.D., Drobnjak, I., Rushworth, M.F.S., Brady, J.M., Smith, S.M., Higham, D.J., Matthews, P.M., 2004. Changes in connectivity profiles define functionally distinct regions in human medial frontal cortex. Proc. Natl. Acad. Sci. USA 101 (36), 13335–13340.

Jung, J., Cloutman, L., Binney, R.J., Lambon Ralph, M.A., 2016. The structural connectivity of higher order association cortices reflects human functional brain networks. Cortex.

Kanwisher, N., McDermott, J., Chun, M.M., 1997a. The fusiform face area: a module in human extrastriate cortex specialized for face perception. J. Neurosci. 17, 4302–4311.

Kanwisher, N., Woods, R.P., Iacobini, M., Mazziotta, J.C., 1997b. A locus in human extrastriate cortex for visual shape analysis. J. Cogn. Neurosci. 9, 133–142.

Kravitz, D.J., Saleem, K.S., Baker, C.I., Mishkin, M., 2011. A new neural framework for visuospatial processing. Nat. Rev. Neurosci. 12 (4), 217–230.

Kriegeskorte, N., Mur, M., Ruff, D.A., Kiani, R., Bodurka, J., Esteky, H., Tanaka, K., Bandettini, P.A., 2008. Matching categorical object representations in inferior temporal cortex of man and monkey. Neuron 60 (6), 1126–1141.

Lambon Ralph M., 2014. Neurocognitive insights on conceptual knowledge and its breakdown. Royal Society Proceedings B, 369(1634), 20120392-20120392.

Lambon Ralph, M.A., Jefferies, E., Patterson, K., Rogers, T.T., 2017. The neural and computational bases of semantic cognition. Nat. Rev. Neurosci. 18, 42–55.

Mantini, D., Vanduffel, W., 2013. Emerging roles of the brain's default network. Neuroscientist 19 (1), 76–87. http://dx.doi.org/10.1177/1073858412446202.

Marinkovic, K., Dhond, R.P., Dale, A.M., Glessner, M., Carr, V., Halgren, E., 2003. Spatiotemporal dynamics of modality-specific and supramodal word processing. Neuron 38 (3), 487–497.

Mesulam, M.M., 1998. From sensation to cognition. Brain 121, 1013–1052.

Mion, M., Patterson, K., Acosta-Cabronero, J., Pengas, G., Izquierdo-Garcia, D., Hong, Y.T., Fryer, T.D., Williams, G.B., Hodges, J.R., Nestor, P.J., 2010. What the left and right anterior fusiform gyri tell us about semantic memory. Brain 133, 3256–3268. http://dx.doi.org/10.1093/brain/awq272.

Molnar-Szakacs, I., Iacoboni, M., Koski, L., Mazziotta, J.C., 2005. Functional segregation within pars opercularis of the inferior frontal gyrus: evidence from fMRI studies of imitation and action observation. Cereb. Cortex 15 (7), 986–994.

Oldfield, R.C., 1971. The assessment and analysis of handedness: the Edinburgh inventory. Neuropsychologia 9 (1), 97–113. http://dx.doi.org/10.1016/0028-3932(71)90067-4.

Pascual, B., Masdeu, J.C., Hollenbeck, M., Makris, N., Insausti, R., Ding, S., Dickerson, B.C., 2013. Large-scale brain networks of the human left temporal pole: a functional connectivity MRI study. Cereb. Cortex 60, bht2.

Patterson, K., Nestor, P.J., Rogers, T.T., 2007. Where do you know what you know? The representation of semantic knowledge in the human brain. Nat. Rev. Neurosci. 8 (12), 976–987. http://dx.doi.org/10.1038/nrn2277.

Plaut, D.C., 2002. Graded modality-specific specialisation in semantics: a computational account of optic aphasia. Cogn. Neuropsychol. 19 (7), 603–639. http://dx.doi.org/10.1080/02643290244000112.

Poser, B.A., Norris, D.G., 2007. Fast spin echo sequences for BOLD functional MRI. Magn. Reson. Mater. Phys. Biol. Med. 20 (1), 11–17. http://dx.doi.org/10.1007/s10334-006-0063-x.

Poser, B.A., Norris, D.G., 2009. Investigating the benefits of multi-echo EPI for fMRI at 7 T. Neuroimage 45 (4), 1162–1172. http://dx.doi.org/10.1016/j.neuroimage.2009.01.007.

Poser, B.A., Versluis, M.J., Hoogduin, J.M., Norris, D.G., 2006. BOLD contrast sensitivity enhancement and artifact reduction with multiecho EPI: parallel-acquired inhomogeneity-desensitized fMRI. Magn. Reson. Med. 55 (6), 1227–1235. http://dx.doi.org/10.1002/mrm.20900.

Power, J.D., Mitra, A., Laumann, T.O., Snyder, A.Z., Schlaggar, B.L., Petersen, S.E., 2014.

Methods to detect, characterize, and remove motion artifact in resting state fMRI. Neuroimage 84, 320–341. http://dx.doi.org/10.1016/j.neuroimage.2013.08.048.

Power, J.D., Schlaggar, B.L., Petersen, S.E., 2015. Recent progress and outstanding issues in motion correction in resting state fMRI. Neuroimage 105, 536–551.

Rauschecker, J.P., Scott, S.K., 2009. Maps and streams in the auditory cortex: nonhuman primates illuminate human speech processing. Nat. Neurosci. 12 (6), 718–724. http://dx.doi.org/10.1038/nn.2331.

Rice, G.E., Hoffman, P., Lambon Ralph, M.A., 2015a. Graded specialization within and between the anterior temporal lobes. Ann. N.Y. Acad. Sci. 1359, 84–97.

Rice, G.E., Lambon Ralph, M.A., Hoffman, P., 2015b. The roles of left versus right anterior temporal lobes in conceptual knowledge: an ALE meta-analysis of 97 functional neuroimaging studies. Cereb. Cortex 25, (4734-4391).

Rice, G., Lambon Ralph, M., Hoffman, P., 2017. Beyond faces: the role of the ventral anterior temporal lobes in transmodal conceptual knowledge for people and other categories. J. Neurosci., (in preparation for publication).

Rozzi, S., Calzavara, R., Belmalih, A., Borra, E., Gregoriou, G.G., Matelli, M., Luppino, G., 2006. Cortical connections of the inferior parietal cortex convexity of the macaque monkey. Cereb. Cortex 16 (10), 1389–1417.

Satterthwaite, T.D., Elliott, M.A., Gerraty, R.T., Ruparel, K., Loughead, J., Calkins, M.E., Eickhoff, S.B., Hakonarson, H., Gur, R.C., Gur, R.E., Wolf, D.H., 2013. An improved framework for confound regression and filtering for control of motion artifact in the preprocessing of resting-state functional connectivity data. Neuroimage 64, 240–256. http://dx.doi.org/10.1016/j.neuroimage.2012.08.052.

Saur, D., Schelter, B., Schnell, S., Kratochvil, D., Küpper, H., Kellmeyer, P., Kümmerer, D., Klöppel, S., Glauche, V., Lange, R., Mader, W., Feess, D., Timmer, J., Weiller, C., 2010. Combining functional and annatomical connectivity reveals brain networks for auditory language comprehension. Neuroimage 49 (4), 3187–3197.

Scott, S.K., Blank, C.C., Rosen, S., Wise, R.J.S., 2000. Identification of a pathway for intelligible speech in the left temporal lobe. Brain 123, 2400–2406. http://dx.doi.org/10.1093/brain/123.12.2400.

Sepulcre, J., Sabuncu, M.R., Yeo, B.T., Liu, H., Jonhnson, K.A., 2012. Stepwise connectivity of the modal cortex reveals the multimodal organization of the human brain. J Neurosci. 32 (31), 10649–10661.

Shi, J., Malik, J., 2000. Normalized cuts and image segmentation. IEEE Trans. Pattern Anal. Mach. Intell. 22 (8), 888–905.

Shimotake, A., Matsumoto, R., Ueno, T., Kunieda, T., Saito, S., Hoffman, P., Kikuchi, T., Fukuyama, H., Miyamoto, S., Takahashi, R., Ikeda, A., Lambon Ralph, M.A., 2014. Direct exploration of the ventral anterior temporal lobe in semantic memory: cortical stimulation and local field potential evidence from subdural grid electrodes. Cereb. Cortex.

Simmons, W.K., Reddish, M., Bellgowan, P.S.F., Martin, A., 2010. The selectivity and functional connectivity of the anterior temporal lobes. Cereb. Cortex 20 (4), 813–825. http://dx.doi.org/10.1093/cercor/bhp149.

Smith, S.M., Fox, P.T., Miller, K.L., Glahn, D.C., Fox, P.M., Mackay, C.E., Filippini, N., Watkins, K.E., Toro, R., Laird, A.R., Beckmann, C.F., 2009. Correspondence of the brain's functional architecture during activation and rest. Proc. Natl. Acad. Sci. USA 106 (31), 13040–13045. http://dx.doi.org/10.1073/pnas.0905267106.

Spreng, R.N., 2012. The fallacy of a "task-negative" network. Front. Psychol., 3. http://

dx.doi.org/10.3389/fpsyg.2012.00145.

Thirion, B., Varoquaux, G., Dohmatob, E., Poline, J.B., 2014. Which fMRI clustering gives good brain parcellations? Front. Neurosci. 8 (167), 1–13.

Tian, B., Reser, D., Durham, A., Kustov, A., Rauschecker, J.P., 2001. Functional specialization in rhesus monkey auditory cortex. Science 292, 290–293.

Ungerleider, L.G., Haxby, J.V., 1994. 'What' and 'where' in the human brain. Curr. Opin. Neurobiol. 4, 157–165.

van den Heuvel, M.P., Sporns, O., 2013. Network hubs in the human brain. Trends Cogn. Sci. 17 (12), 683–696.

Van Dijk, K.R.A., Sabuncu, M.R., Buckner, R.L., 2012. The influence of head motion on intrinsic functional connectivity MRI. Neuroimage 59 (1), 431–438. http://dx.doi.org/10.1016/j.neuroimage.2011.07.044.

Vincent, J.L., Kahn, I., Snyder, A.Z., Raichle, M.E., Buckner, R.L., 2008. Evidence for a frontoparietal control system revealed by intrinsic functional connectivity. J. Neurophysiol. 100 (6), 3328–3342. http://dx.doi.org/10.1152/jn.90355.2008.

Visser, M., Jefferies, E., Embleton, K.V., Lambon Ralph, M.A., 2012. Both the middle temporal gyrus and the ventral anterior temporal area are crucial for multimodal semantic processing: distortion-corrected fMRI evidence for a double gradient of information convergence in the temporal lobes. J. Cogn. Neurosci. 24 (8), 1766–1778.

Visser, M., Lambon Ralph, M.A., 2011. Differential contributions of bilateral ventral anterior temporal lobe and left anterior superior temporal gyrus to semantic processes. J. Cogn. Neurosci. 23 (10), 3121–3131. http://dx.doi.org/10.1162/jocn_a_00007.

von Luxburg, U., 2007. A tutorial on spectral clustering. Stat. Comput. 17 (4), 395–416.

Vossel, S., Geng, J.J., Fink, G.R., 2014. Dorsal and ventral attention systems: distinct neural circuits but collaborative roles. Neuroscientist 20 (2), 150–159.

Weissenbacher, A., Kasess, C., Gerstl, F., Lanzenberger, R., Moser, E., Windischberger, C., 2009. Correlations and anticorrelations in resting-state functional connectivity MRI: a quantitative comparison of preprocessing strategies. Neuroimage 47 (4), 1408–1416. http://dx.doi.org/10.1016/j.neuroimage.2009.05.005.

Wig, G.S., Laumann, T.O., Petersen, S.E., 2014. An approach for parcelling human cortical areas using resting-state correlations. Neuroimage 93 (2), 276–291.

Xiang, H.-D., Fonteijn, H.M., Norris, D.G., Hagoort, P., 2010. Topographical functional connectivity pattern in the perisylvian language networks. Cereb. Cortex 20 (3), 549–560. http://dx.doi.org/10.1093/cercor/bhp119.

Yan, C.G., Cheung, B., Kelly, C., Colcombe, S., Craddock, R.C., Di Martino, A., Li, Q.Y., Zuo, X.N., Castellanos, F.X., Milham, M.P., 2013. A comprehensive assessment of regional variation in the impact of head micromovements on functional connectomics. Neuroimage 76 (1), 183–201. http://dx.doi.org/10.1016/j.neuroimage.2013.03.004.

Yeo, B.T.T., Krienen, F.M., Sepulcre, J., Sabuncu, M.R., Lashkari, D., Hollinshead, M., Roffman, J.L., Smoller, J.W., Zöllei, L., Polimeni, J.R., Fischl, B., Liu, H., Buckner, R.L., 2011. The organization of the human cerebral cortex estimated by intrinsic functional connectivity. J. Neurophysiol. 106 (3), 1125–1165.

Zuo, X.N., Ehmke, R., Mennes, M., Imperati, D., Castellanos, F.X., Sporns, O., Milham, M.P., 2012. Network centrality in the human functional connectome. Cereb. Cortex 22 (8), 1862–1875. http://dx.doi.org/10.1093/cercor/bhr269.